Semiconductor Physics, Quantum Electronics & Optoelectronics, 2005. V. 8, N 4. P. 95-104.

PACS 81.05.Rm

Porous nanostructured InP: technology, properties, application

I.N. Arsentyev[1], A.B. Bobyl[1], S.G. Konnikov[1], I.S. Tarasov[1], V.P. Ulin[1], M.V. Shishkov[1], N.S. Boltovets[2], V.N. Ivanov[2], A.E. Belyaev[3], R.V. Konakova[3], Ya.Ya. Kudryk[3], A.B. Kamalov[3], P.M. Lytvyn[3], E.P. Markovskiy[3], V.V. Milenin[3], R.A. Red'ko[3]
[1]A.F. Ioffe Physico-Technical Institute of RAN, 26, Politekhnicheskaya str., St.-Petersburg, 194021, Russia
E-mail: arsentyev@mail.ioffe.ru; phone: +7-812-247-91-34
[2]State Enterprise Scientific & Research Institute "Orion",
8a, Eugene Pottier str.,03057 Kyiv, Ukraine
E-mail: bms@i.kiev.ua; phone: +380-44-456-05-48
[3]V. Lashkaryov Institute of Semiconductor Physics, NAS of Ukraine,
45, prospect Nauky, 03028 Kyiv, Ukraine
E-mail: konakova@isp.kiev.ua; phone: +380-44-525-61-82

Abstract. We prepared porous InP (100) substrates with a nanostructured surface relief on which InP epitaxial films were grown. The structure, morphological, and photoluminescence properties of nanostructured substrates and InP epilayers grown on them were studied. These InP epilayers grown on the porous and standard InP substrates were used to make microwave diodes. We showed the advantages of the diodes made on the porous substrates (over those made on the standard ones) caused by higher structural perfection of the InP epilayers grown on the porous substrates.

Keywords: porous InP, InP epilayers, photoluminescence, Schottky-barrier diode, Gunn diode.

Manuscript received 19.09.05; accepted for publication 25.10.05.

1. Introduction

Indium phosphide attracts attention of the developers of microwave active elements because this semiconductor material has higher capabilities than gallium arsenide [1-3]. They become apparent in the features of its band structure that ensure higher (than in GaAs) values of threshold field, maximal drift velocity and saturation velocity in strong fields. Besides, its thermal conductivity is over that of GaAs. Just these parameters point at the possibility of InP application for fabrication of microwave diodes (in particular, the Gunn diodes) that could operate over the whole millimeter wavelength range [1].

Besides, it is known that production of such diodes requires uniform structurally perfect semiconductor material with minimal density of strain concentrators [4]. To obtain indium phosphide meeting the above requirements is a difficult physical and technological problem and remains problematic up to now.

At the same time, in recent years a comparatively novel approach to formation of structurally perfect semiconductor films has been developed. In this approach, textured and porous semiconductor growth surfaces are used as a substrate material [5-11]. It should be noted that the first report on application of porous substrate (GaAs) for epitaxial film formation was made in the work [5] that was carried out at the A.F. Ioffe Physico-Technical Institute of RAN. And in [12] the possibility for InP epitaxial film growth on porous InP substrate was shown. In both cases the GaAs and InP porous substrates take over elastic strains that appear in the course of epitaxial film growth and further cooling process. Another feature of such substrates is that their developed surfaces serve as a high-capacity dislocation drain. This fact offers a real possibility for improvement of structural perfection of epitaxial layers.

In what follows, we consider obtaining the porous indium phosphide and investigation of some of its properties, as well as its application as a substrate material in the course of formation of InP epitaxial layers using the liquid-phase epitaxy (LPE) technique and development of microwave diodes on their basis.

2. Preparation of porous indium phosphide

We used single-crystalline *n*-type indium phosphide wafers as a substrate material. They had crystallographic

© 2005, V. Lashkaryov Institute of Semiconductor Physics, National Academy of Sciences of Ukraine

orientation (100) (with an accuracy of 20 arc seconds) and were doped with tin (up to the concentration of 2×10^{18} cm^{-3}). After mechanical grinding and lapping, the wafers were exposed to chemical etching (to remove a disordered surface layer). Pre-growth treatment was performed according to the technique described in [13]. On the whole, the process of substrate preparation before epitaxy involved the following operations:

- wafer surface degreasing in organic solvents (such as ethanol, acetone, and carbon tetrachloride);
- treatment in polishing etchant (a mixture of HBr and saturated water solution of $K_2Cr_2O_7$, with volume ratio of 1:1) at room temperature (operating side down), with intense mixing for 30 s;
- thorough washing from the etchant in cold distilled water;
- treatment in H_3PO_4 for 2 min (operating side up) to remove Br ions from the surface;
- washing in distilled water;
- centrifugal drying of the substrate.

The substrates prepared in the above way were used for both pore formation and growing of the reference samples on the "rigid" substrate.

The porous material interlayers were formed in the course of anodic electrochemical process (a scheme of the facility for preparation of porous substrates is shown in Fig. 1). The pulsed voltage (frequency of 2 Hz) was applied to the cell according to the technique described in [14].

The anode was a metallic tube, with one end (operating) treated with pure indium to improve the adhesion and contact properties, while another end was connected to a jet pump to ensure underpressure. The substrate prepared in the above way was placed on the anode operating contact, with its back side oriented to the contact. The anode was positioned so that the substrate operating surface was in contact with the electrolyte meniscus.

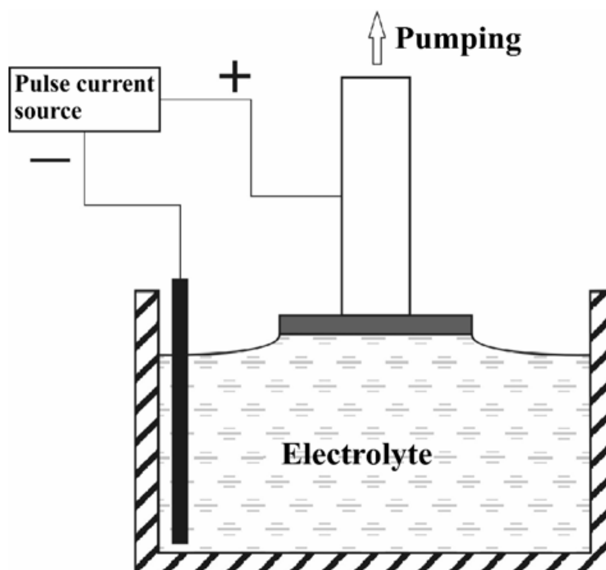

Fig. 1. Scheme of the facility for preparation of porous substrates.

Water solutions of fluorides (NH_4F + HF), chlorides (NH_4Cl + HCl) and bromides (KBr + HBr) served as electrolytes. The pulse voltages applied to the cell (7−10 V) were several times higher than the threshold voltages of pore formation; the process duration was 20−25 s.

The porous layers obtained in the fluoride electrolyte involved 30−50 nm channels of triangular section. These channels penetrated and branched in the crystal bulk along the direction ⟨111⟩ B.

The pores obtained in the above treatment modes (in chloride and bromide electrolytes) had a trend to propagate along the electric field (at a normal to the crystal surface), without any preferred crystallographic orientation. The pore size was close to that in the fluoride layers. Such configuration of pores growing from the surface (100) results from superposition of their motions along the directions ⟨111⟩ A and ⟨111⟩ B.

The pore volume is filled with the products of partial oxidation of InP. They appear as a result of InP reaction with the anion components of solutions according to the mechanism of nucleophilic substitution. The initial composition of these products is $InPX_{2+n}$ (with $n > 2$ and X = F, Cl, Br). In the course of pore formation, the reaction products serve as a solid electrolyte that ensures transport of the adsorbing anions to the reaction front at the pore bottom. One cannot exclude subsequent decomposition of the products left in the pores with production of atomic phosphorus and trihalides (and, maybe, more composite mixed halides) retaining the In–P bonds.

The substrates formed in chloride electrolyte were used for growth processes because they demonstrated better repeatability.

3. Properties of porous indium phosphide

When studying porous sublayer configuration, we applied scanning electron microscopy (SEM) and atomic force microscopy (AFM). Shown in Fig. 2 is a SEM pattern of a chip of porous InP (100) substrate obtained using the above technology. One can see a clearly pronounced structure of porous sublayer (which is a system of pores and partition walls). The preferred direction of pore formation is normal to the surface. A branchy pore structure is distinct. One can see that the density of channels is distributed very uniformly over the whole formed sublayer, and the sublayer−crystal bulk interface is practically flat. The pores make a regular network whose horizontal (vertical) period is 130 (200) nm (Fig. 3). The pore size dispersion is rather small.

The results of our AFM studies confirmed the above fact and enabled us to determine an approximate law of pore size distribution shown in Fig. 4. These facts

© 2005, V. Lashkaryov Institute of Semiconductor Physics, National Academy of Sciences of Ukraine

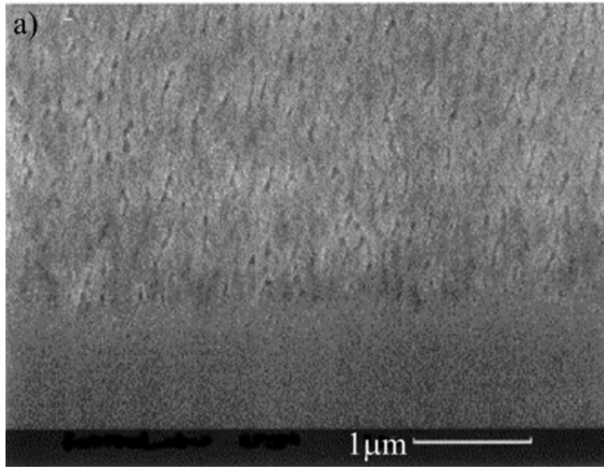

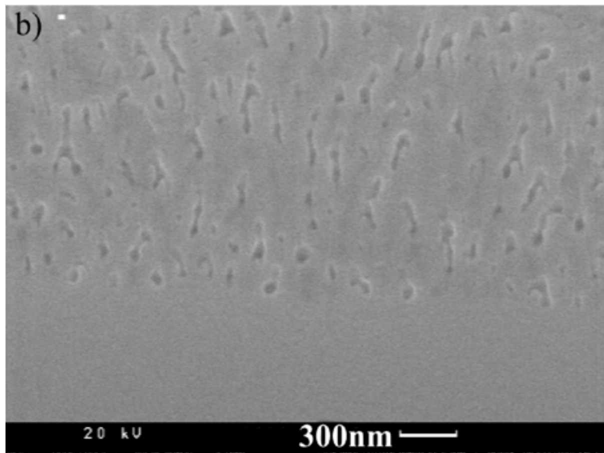

Fig. 2. A formed porous layer on the InP substrate (chip): a – the porous sublayer-crystal bulk interface; b – pore geometry (enlarged).

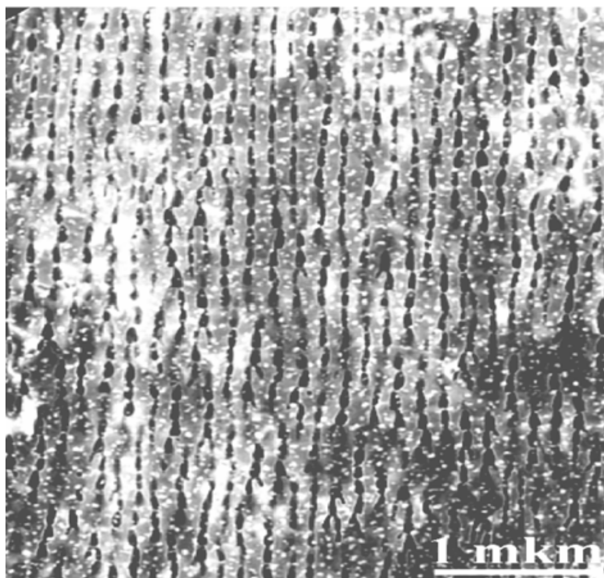

Fig. 3. A pattern of porous substrate surface.

(i) make it possible to state that the porous sublayer is a practically uniform system that takes strains away, and (ii) confirm the possibility of obtaining the heterostructures quality of which exceeds that of the traditional LPE-grown structures.

Our studies of the substrate surface with a formed porous sublayer showed that the initial singular face surface was practically lost. It was replaced by a system of vicinal hillocks. A microrelief of porous substrate is shown in Fig. 5. Due to such surface structure (with plenty of elementary steps), growth of epitaxial layer at initial stages occurs according to the mechanism of embedding of adsorbed components in the growth steps available at the surface (without formation of individual nuclei of a new phase). This reduces the activation energy of nucleation. At the same time, this results in increase of the defect density in the layer grown immediately on the porous substrate, thus leading to the necessity of InP buffer layer growth directly on the porous substrate to ensure synthesis of a high-quality heterostructure.

To reveal the features of the surface recombination processes at the surfaces that restricted pore channels, we performed photoluminescence (PL) investigations of porous substrates without epitaxial layers. Fig. 6 demonstrates PL spectra of porous and continuous indium phosphide. The spectral curve corresponding to non-annealed InP sample with a formed porous sublayer is of noise character. This fact, along with the SEM data (Fig. 2), makes it possible to state that both the sample surface and porous sublayer bulk are passivated with the products of electrochemical oxidation.

The spectral curve of the sample exposed to low-temperature annealing (2 h in the hydrogen atmosphere at $T = 250$ °C) has a peak at lower energies (about 1.26–1.27 eV) than the reference sample (continuous substrate, bandgap $E_g = 1.4$ eV). This rather intense peak

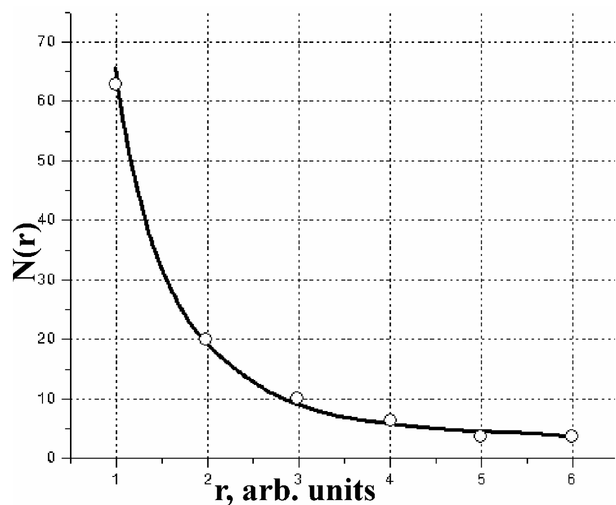

Fig. 4. The law of pore size distribution.

© 2005, V. Lashkaryov Institute of Semiconductor Physics, National Academy of Sciences of Ukraine

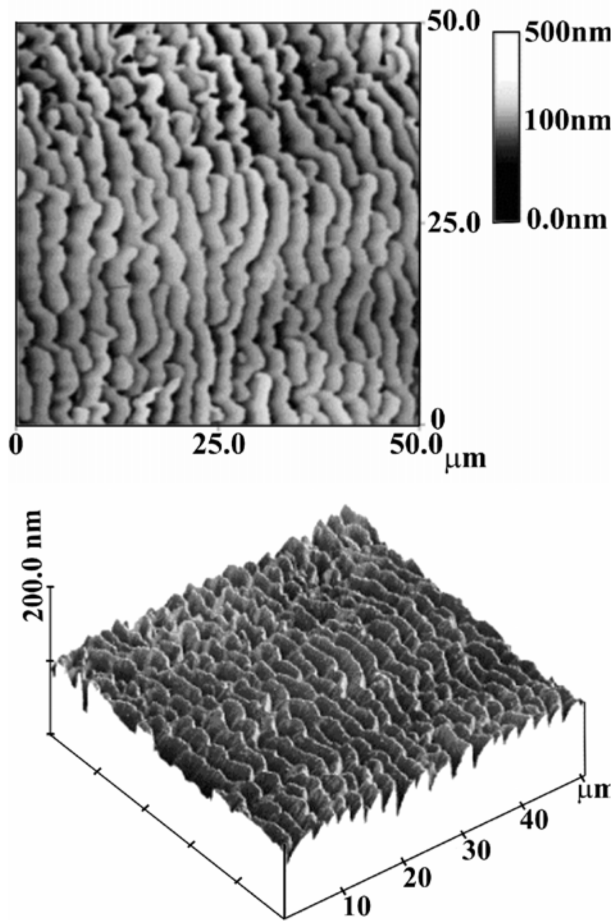

Fig. 5. A porous substrate microrelief.

has the big (106 meV) half-width. A considerable peak energy decrease can be explained (in the case of its interband origin) by presence of a high density of localized states in the bandgap (over the valence band top E_v). This decreases the porous InP bandgap value. Absence of the principal band in the PL spectrum of porous InP may be due to absorption of radiation in the porous sublayer bulk and re-emission via the formed levels in the bandgap [15].

The X-ray experiments also revealed some features inherent to the porous material itself. The X-ray diffraction reflection curve of porous indium phosphide is shown in Fig. 7. Along with a narrow peak (due to high-degree structural perfection of the monocrystalline substrate), the rocking curve has additional peaks. This spectrum broadening results from interference of the main radiation (reflected from crystallographic planes) and radiation from the planes restricting the pore channels.

The latter planes have the properties of partially polycrystalline material, because, while having, on the whole, the same orientation, they are, however, the result of pore motion along the directions ⟨111⟩ A and ⟨111⟩ B. So, they demonstrate some misorientation relatively to each other, as well as to the principal crystallographic directions.

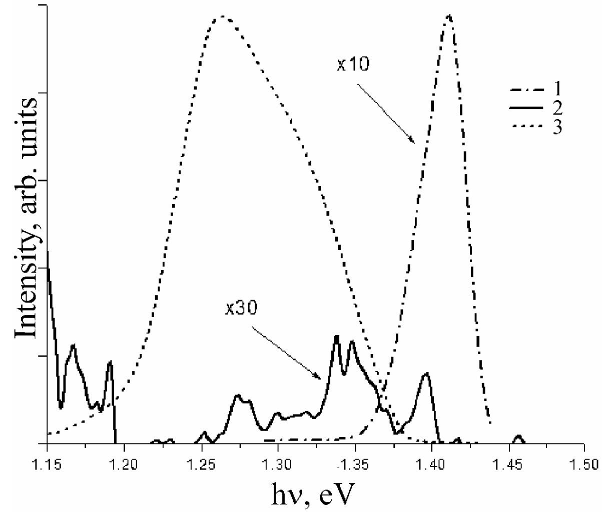

Fig. 6. PL spectra of porous InP (77 K): 1 – of the standard “rigid” InP substrate; 2 – of porous InP (initial); 3 – of porous InP after low-temperature annealing.

The effect of PL spectrum broadening is caused by the fact that, near the InP reflection (004), the diffraction curves for the samples grown on porous substrates are superposition of the coherent components of diffracted radiation from the monocrystalline part of InP substrate and the components of the porous part of InP substrate that is disordered by the pores. To separate the contributions from the above components, we took the rocking curves near the InP reflection (311). The diffraction from porous substrates has two peaks: one (with FWHM of about 54 arc seconds) is related to a thin (< 100 nm) near-surface region of the porous InP substrate, while another (with FWHM of about 300 arc seconds) is related to the bulk part of the porous InP substrate with a developed system of branchy pores. The interval between the peaks is 540 arc seconds. This corresponds to mismatch of lattice parameters of these layers $\Delta a/a \sim 5\times10^{-3}$ [12].

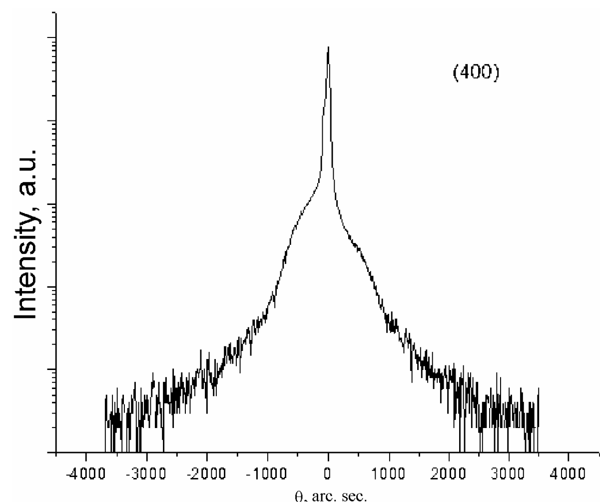

Fig. 7. A diffraction reflection curve of porous InP.

© 2005, V. Lashkaryov Institute of Semiconductor Physics, National Academy of Sciences of Ukraine

4. Properties of the epitaxial indium phosphide layer

It was necessary to apply a buffer layer when growing the heterostructures. So, we shall consider briefly the properties of these structures.

The quality of grown structures was controlled from the PL data. Shown in Fig. 8 is PL spectrum of epitaxial indium phosphide on the porous substrate at a high level of excitation. It involves a broad low energy peak due to the porous sublayer, similarly to the spectrum in Fig. 6.

Let us compare the properties of epitaxial layers grown (under the same technological conditions) on porous and continuous substrates. A comparison spectrum is shown in Fig. 9. The parameters of the corresponding layers are given in Fig. 10 and Table 1.

The principal PL band of the sample grown on the porous substrate has a smaller half-width in comparison with the traditional composition. This indicates higher quality of the grown layer. The positions of the additional PL bands (caused by the impurity level) are the same. However, a distinction in their intensities requires further consideration. It seems that higher intensity of the impurity peak is related to a big amount of the background impurities in the crystallized layer [16].

Table 1. Parameters of the InP homoepitaxial layers determined from the PL data.

Type of substrate	Principal PL band, eV	Half-width of the principal peak, meV	Additional PL band, eV	Layer thickness, μm
continuous	1.41	16.6	1.375	1.68
porous	1.41	12.7	1.378	2.01

The difference in the layers thicknesses is due to different growth mechanisms. For the porous layers, this mechanism is close to the screw one that is typical of atomically-rough faces, while for the continuous layers the growth is proceeding layer-by-layer, because the face is atomically-flat.

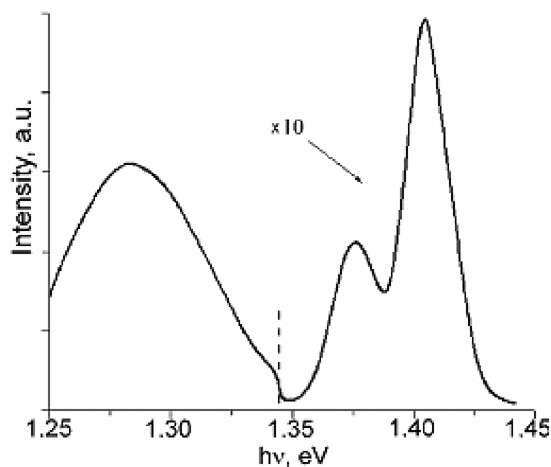

Fig. 8. PL spectrum of epitaxial InP on porous substrate with grown buffer layer (77 K): porous substrate – $h\nu$ = 1.28 eV; ΔE = 60 meV; epitaxial layer – $h\nu$ = 1.40 eV; ΔE = 11 meV.

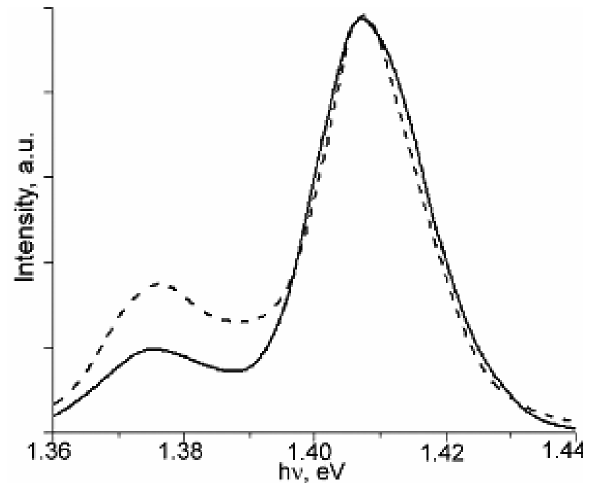

Fig. 9. PL spectra of InP epitaxial layers (77 K) grown on "rigid" (1) and porous (2) substrate: 1 – $h\nu$ = = 1.41 eV, ΔE = 16.6 meV; 2 – $h\nu$ = 1.41 eV, ΔE = 12.7 meV.

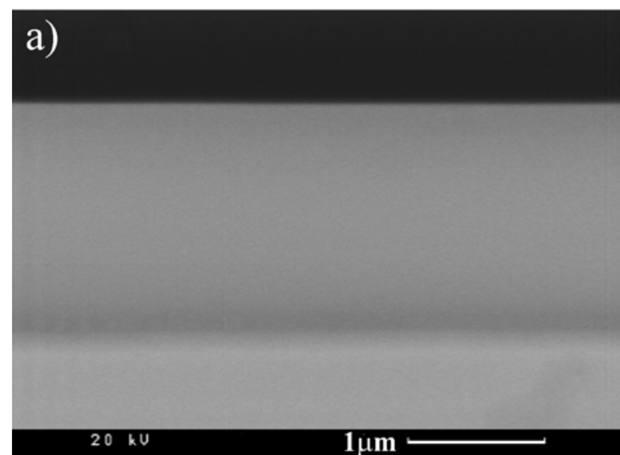

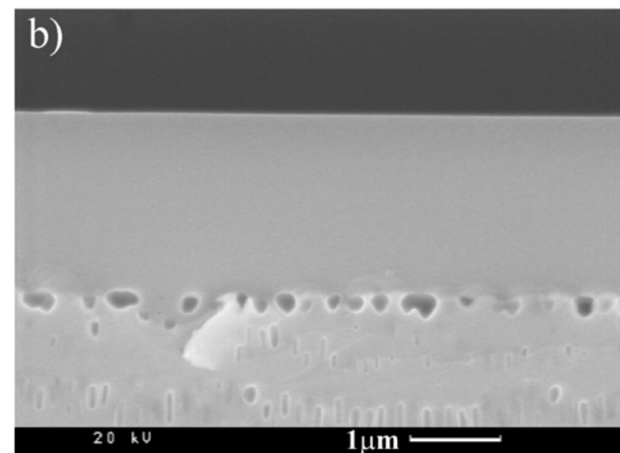

Fig. 10. Chips: epitaxial InP layers on "rigid" (a) and "porous" (b) substrates.

© 2005, V. Lashkaryov Institute of Semiconductor Physics, National Academy of Sciences of Ukraine

5. Properties of the Schottky-barrier diode structures made on the porous InP substrates

The Au−TiB−n^{++}-InP diodes (400 μm in diameter) were made using the magnetron sputtering of TiB_x and Au followed with photolithography. The ohmic contacts were formed using the magnetron sputtering of Ge, Au and TiB_x layers and their firing in the hydrogen atmosphere at $T = 500$ °C for 1 min. We measured $I-V$ curves of the diode structures at room temperature; from them, we calculated the Schottky barrier height φ_B and ideality factor n. The diodes were made on the standard "rigid" epiready InP (100) substrate (concentration of tin impurity was $\sim 2\times10^{18}$ cm^{-3}) and three other substrates of the same type, but with a formed porous layer (Table 2).

Table 2. Parameters of the porous InP layers.

Type of substrate	Technology of pore formation	Porous layer thickness, μm	Note
InP A0	-	-	initial rigid epiready substrate
InP A1	chloride	8−10	
InP A2	chloride	16−18	
InP A3	fluoride	15	

The histograms of φ_B and n values in each of the above wafers obeyed the Gaussian law. It was found that in the Schottky-barrier diodes (SBDs) made on the porous substrates InP A2 and InP A3 (porous layer thicknesses of which were 1.5−2 times large than those of the InP A1 substrate) the average statistical spread of φ_B (n) values was by 0.07 eV (0.1) less than in the diodes made on the epiready and InP A1 substrates. This fact confirms the SEM results that the porous sublayer is practically uniform system.

Shown in Fig. 11 are the histograms of φ_B values on the initial epiready and porous InP A2 substrates. From them, one can also see that φ_B is distributed more uniformly over the porous substrate than over the initial epiready one. This seems to be related to removal of the most imperfect areas in the InP bulk in the course of pore formation.

6. Properties of the Schottky-barrier diode structures made on epilayers grown on the porous InP substrates

The SBD structures Au−TiB_x−n-n^+-n^{++}-InP were made as forward mesas. An area of wafer with such structures is shown in Fig. 12. The TiB_x and Au layers were formed using the magnetron sputtering.

We used the Auger electron spectroscopy (AES) to obtain component concentration depth profiles in the barrier-forming TiB_x-n-n^+-n^{++}-InP contacts formed on the device structures that were prepared on the porous and standard "rigid" InP substrates. It was found that, in the first case (porous substrate), the TiB_x−InP interface was more abrupt than in the standard device structure. This is in agreement with the barrier contact parameters calculated from the experimental $I-V$ curves [17].

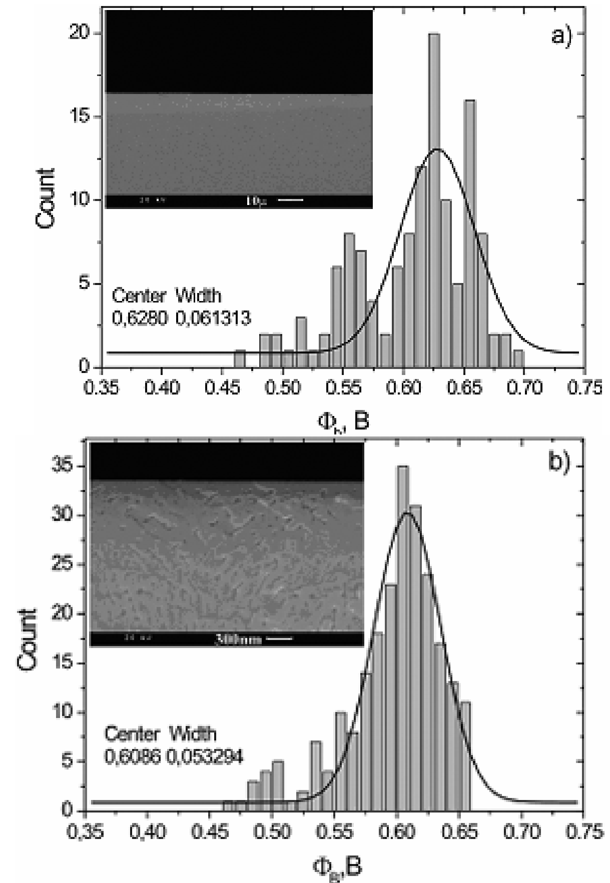

Fig. 11. Histograms of φ_B on the initial epiready InP substrate (a) and porous InP A2 substrate (b) (inset - chips of the corresponding substrates).

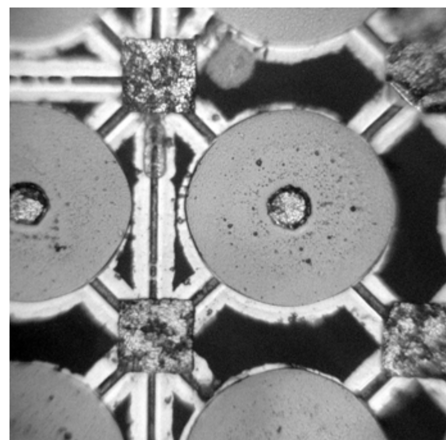

Fig. 12. An area of technological wafer with Au−TiB_x−n-n^+-n^{++}-InP SBD structures made using the basic process of the State Enterprise SRI "Orion" (mesa diameter is 40 μm).

© 2005, V. Lashkaryov Institute of Semiconductor Physics, National Academy of Sciences of Ukraine

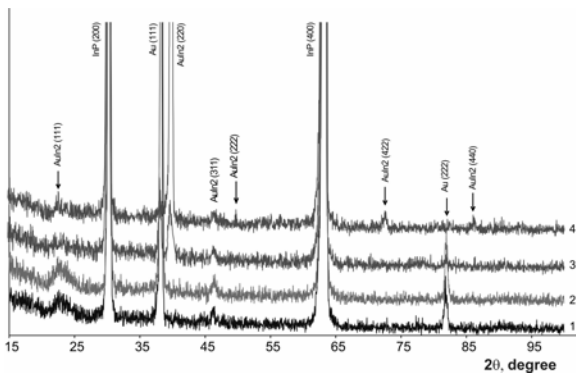

Fig. 13. X-ray diffraction patterns of Au−TiB$_x$−Au contacts: 1 – initial sample; 2, 3 and 4 - after RTA at T = 300, 400 and 600 °C, respectively.

The ohmic contacts to the diode structures of both types were made on the basis of Au−TiB$_x$−Au metallization using the magnetron sputtering of the corresponding contact components onto the InP substrates heated up to 200 °C. Shown in Fig. 13 are the X-ray diffraction patterns taken for the initial sample and those exposed to rapid thermal annealing (RTA) at T = 300, 400 and 600 °C. One can see that in the non-annealed sample (curve 1 in Fig. 13) the gold film crystallites are oriented in the plane (111), the TiB$_x$ layer is quasi-amorphous, and $AuIn_2$ traces are also observed. RTA at T = 300 °C (curve 2) doesn't change the phase composition of the system contacts. After RTA at T = 400 °C (curve 3), the gold drops abruptly (while texturing remains the same) and the amount of $AuIn_2$ increases.

After RTA at T = 600 °C (curve 4), the signal from pure gold decreases abruptly, and the amount of polycrystalline $AuIn_2$ phase (with predominant crystallite orientation along (220)) increases. The crystal structure of TiB$_x$ doesn't change: it remains quasi-amorphous after all RTA performed. These results correlate with the Auger concentration depth profiles of the contact components in the studied systems, taken before and after RTA (see Fig. 14). Indeed, the profiles practically did not change in the initial sample and that annealed at 300 °C (Fig. 14a, b). Contrary to this, RTA at T = 400 (600) °C led to considerable changes at the Au−InP interface related to the intense phase formation. Contact resistivity ρ_c in the initial sample and those after RTA at 300 °C was ~ $(1…2)\times10^{-3}$ Ohm·cm^2, while after RTA at T = 400 °C it was ~ $(0.8…2)\times10^{-4}$ Ohm·cm^2. RTA at 600 °C increased ρ_c by more than an order of magnitude in comparison with the value after RTA at T = 400 °C.

The above results concerning the ρ_c variations can be explained by taking into account formation of a developed relief on the semiconductor substrate surface due to the intense phase formation (say, as a result of RTA at T = 400 °C). It is known that this determines the non-polar mechanism of current flow in the contact and leads to both increase of the generation-recombination processes at current flow and formation of ohmic contacts.

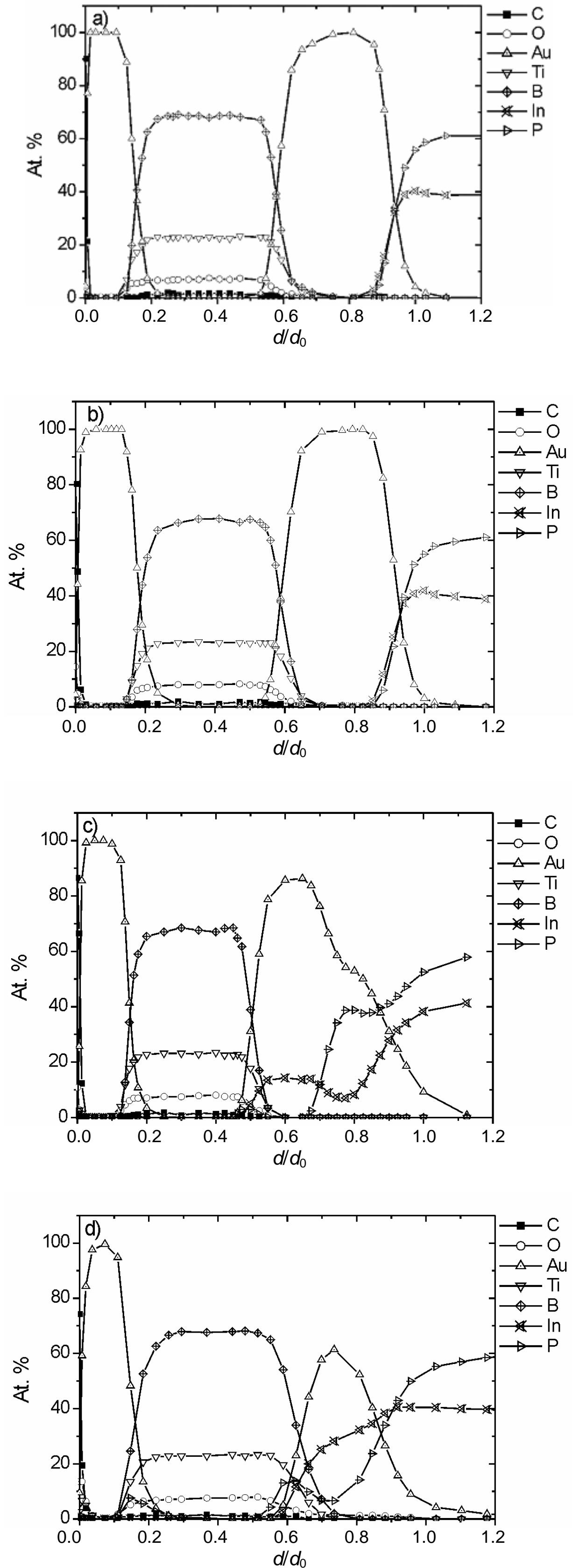

Fig. 14. Component distribution profiles in Au−TiB$_x$−Au contacts: a – initial sample; b, c and d – after RTA at T = 300, 400 and 600 °C, respectively.

© 2005, V. Lashkaryov Institute of Semiconductor Physics, National Academy of Sciences of Ukraine

Since the Schottky barriers were made as forward mesas, and the ohmic contact was formed to the back side of the wafer, no essential distinctions in structure, phase formation and ohmic contact properties were found between the standard samples and those made on the porous substrate. However, $I-V$ curves of different SBDs (made on epilayers grown on the standard "rigid" and porous InP substrates) differ essentially. In both cases, the main mechanism of current flow corresponding to the forward branches of $C-V$ curves is thermal emission. This is evidenced by small values of the ideality factor ($n \sim 1.08\ldots1.1$ in both cases). However, the SBDs made on the standard substrates have an excess current component in the 0.03…0.2 V forward bias (this component values differ considerably in different samples). Contrary to this, no such component exists in the samples made on the porous substrates. This agrees with the previously published results [11] of measurements of $I-V$ curves for diodes with Au−Ti Schottky barrier made on the InP epilayers grown under similar conditions on porous substrates. An excess current component was observed also on the back $C-V$ curves branch in the diode structures on the standard substrates. It decreased essentially in the diode structures formed on the epilayers grown on the porous substrates. In this case, one can observe even avalanche breakdown that corresponds to the impurity concentration in the epistructure.

An analysis of $C-V$ curves shows that the observed changes of leakage currents seem to result from the structure-impurity nonuniformities existing in the standard device structures. However, in the course of porous substrate formation, the most imperfect areas are being etched-off. This increases the degree of structure uniformity of formed InP growth surface, thus improving the electrophysical properties of epilayers (this is in agreement with the above PL data). The typical forward and reverse branches of $I-V$ curves of the Au−TiB_x−n-n^+-n^{++}-InP diode structures made on the standard and porous InP substrates are given in Fig. 15.

7. The features of the electrical characteristics of the Gunn diodes on epilayers formed on the porous InP substrates

The Gunn diode models were made (according to the basic process of the State Enterprise SRI "Orion") on the InP epilayers grown on the standard and porous substrates, with ohmic contacts Au−TiB_x−AuGe (the contact resistivity was $\leq 10^{-5}$ Ohm·cm^2). In both cases, we used the epistructures in which the substrate thickness was ~350 µm and impurity (tin) concentration was $\sim 2\times10^{18}$ cm^{-3}. The buffer layer had the thickness of ~3 µm and impurity concentration of $\sim (5\ldots6)\times10^{17}$ cm^{-3}. The active layer was 2 µm thick; its impurity concentration was $\sim 10^{16}$ cm^{-3}. The mesa diameter was ~ 60 µm. An area of technological wafer with the Gunn diode chips is shown in Fig. 16.

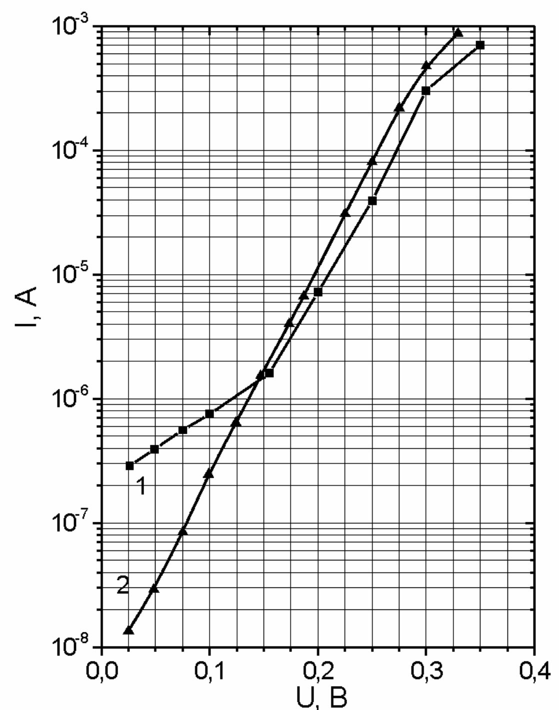

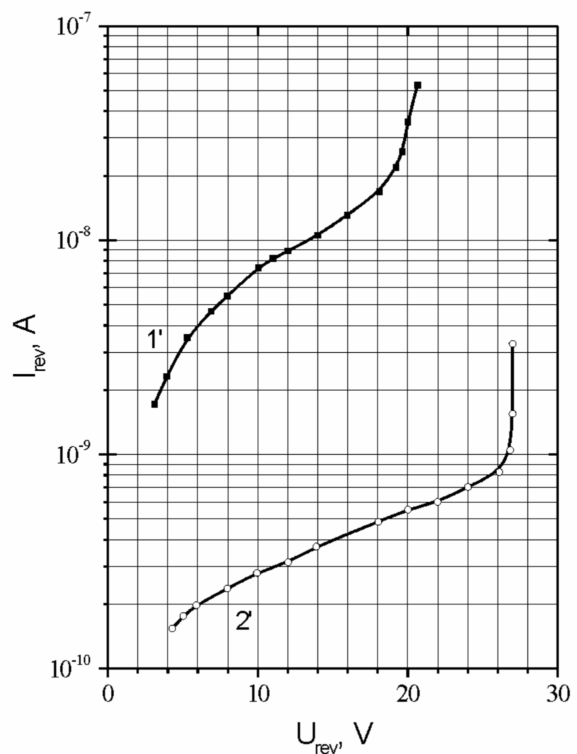

Fig. 15. Forward (a) and reverse (b) branches of $I-V$ curves for Au−TiB_x−n-n^+-n^{++}-InP SBDs made on the standard "rigid" (curves 1 and 1′) and porous (curves 2 and 2′) substrates. Curves 1 and 2 (1′ and 2′) – the forward (reverse) branches of $I-V$ curves.

© 2005, V. Lashkaryov Institute of Semiconductor Physics, National Academy of Sciences of Ukraine

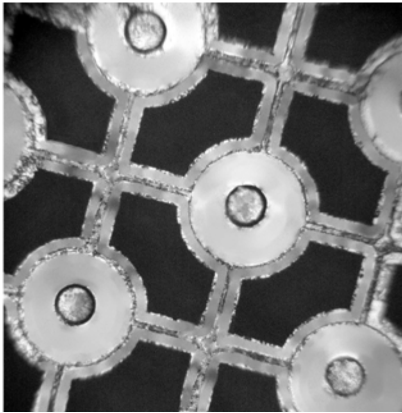

Fig. 16. Part of the technological wafer with the Gunn diode chips.

The diode chips were assembled in metal-quartz packages. The measurement of microwave parameters in the 118−150 GHz frequency range was made in a rectangular (0.8×1.6 mm) waveguide oscillator. The maximal power output at a frequency of 120 GHz (the second harmonic) was ~ 3.5…4 mW. It was found also that the oscillators with the diodes made on the porous substrate began to oscillate at operating voltages close to the threshold ones. And in the ordinary Gunn oscillators made on the standard InP substrates, the generation of microwave oscillations appears at operating voltages 20 % over the threshold ones.

8. Conclusion

The results of our structural, photoluminescence and electrophysical investigations of (i) the nanostructured InP substrates, (ii) epilayers grown on them, and (iii) microwave diodes formed on these epilayers have demonstrated a real possibility of development of structurally perfect InP epitaxial layers of device quality.

Acknowledgements

The work was made in the framework of the Russia−Ukraine Program on Nanophysics and Nanoelectronics.

References

1. A.S. Tager, Prospects of indium phosphide application in the semiconductor microwave electronics, in: *Indium phosphide application in semiconductor electronics*, ed. S.I. Radautsan. Shtiintsa, Kishinev (1988) p. 120-132 (in Russian).
2. V.G. Bozhkov, V.S. Lukash, Semiconductor microwave devices // *Vestnik Tomskogo Gosudarstvennogo Universiteta, Ser. Fizika* No 285, p. 129-138 (2005) (in Russian).
3. Dargys, J. Kundrotas, *Handbook of physical properties of Ge, Si, GaAs and InP*. Science and Encyclopedia Publishers, Vilnius (1994).
4. M.V. Ardyshev, V.M. Ardyshev, Characteristics of gallium arsenide Gunn structures and Gunn devices on their basis made using radiation-thermal technology // *Fiz. Tekhn. Poluprov*. **37**(4), p. 456-459 (2003) (in Russian).
5. V.V. Mamutin, V.P. Ulin, V.V. Tretyakov, S.V. Ivanov, S.G. Konnikov, P.S. Kopiev, Obtaining of cubic GaN with molecular-beam epitaxy on porous GaAs substrates // *Pis'ma v ZhTF*. **25**(1), p. 3-9 (1999) (in Russian).
6. F.Yu. Soldatenkov, V.P. Ulin, A.A. Yakovenko, O.M. Fedorova, S.G. Konnikov, V.I. Korolkov, Unstrained epitaxial films of $In_xGa_{1-x}As$ formed on porous GaAs // *Pis'ma v ZhTF* **25**(21), p. 15-20 (1999) (in Russian).
7. Yu.N. Buzynin, S.A. Gusev, V.M. Daniltsev, M.N. Drozdov, A.V. Murel, O.I. Khrykin, V.I. Shashkin, Single-crystalline layers of GaAs, AlGaAs and InGaAs formed with LPE technique from metal-organic compounds on porous gallium arsenide substrates // *Pis'ma v ZhTF* **26**(7), p. 64-69 (2000) (in Russian).
8. A.A. Akopyan, O.Yu. Borkovskaya, N.L. Dmitruk, A.V. Karimov, R.V. Konakova, V.V. Milenin, A.V. Sachenko, M.N. Tursunov, D.M. Yodgorova, *Photoconverters with AlGaAs/GaAs heterojunction on textured GaAs substrates (Physico-technological aspects)*. Fan Publishers, Tashkent (2004).
9. A.A. Sitnikova, A.V. Bobyl, S.G. Konnikov, V.P. Ulin, Peculiarities of epitaxial film formation on porous $A^{III}B^{V}$ substrates // *Fiz. Tekhn. Poluprov*. **39**(5), p. 552-556 (2005) (in Russian).
10. N.S. Savkina, V.V. Ratnikov, V.B. Shuman. Effect of high-temperature epitaxial process of SiC layer growth on the structure of porous silicon carbide // *Fiz. Techn. Poluprov*. **35**(2), p. 159-163 (2001) (in Russian).
11. I.L. Shulpina, V.V. Ratnikov, N.S. Savkina, V.B. Shuman. X-ray diffraction study of the actual structure of homoepitaxial layers grown on porous 6H- and 4H-SiC substrates // *Poverkhnost*' No 6, p.18-22 (2005) (in Russian).
12. I.N. Arsentyev, M.V. Baydakova, A.V. Bobyl, L.S. Vavilova, S.G. Konnikov, V.P. Ulin, N.S. Boltovets, R.V. Konakova, V.V. Milenin, D.I. Voitsikhovskyi, Structural and electrical characteristics of InP epitaxial layers on porous substrates and parameters of Au−Ti Schottky barriers to them // *Pis'ma v ZhTF* **28**(17), p. 57-66 (2002) (in Russian).
13. A.V. Ovchinnikov, *Ph.D. Thesis*, The development of liquid-phase manufacturing technology for InGaAs/InP (λ = 1.3 μm) laser structures (for FOCL) with ultra-thin active areas. Leningrad, A.F. Ioffe Physico-Technical Institute of RAN (1988) (in Russian).
14. S. Langa, I.M. Tiginyanu, J. Carstensen, M. Christophersen, H. Fölla, Formation of porous layers with

© 2005, V. Lashkaryov Institute of Semiconductor Physics, National Academy of Sciences of Ukraine

different morphologies during anodic etching of *n*-InP // *Electrochem. Solid-State Lett*. **3**(11), p. 514-516 (2000).
15. E.P. Domashevskaya, V.A. Terekhov, V.M. Kashkarov, S.Yu. Turischev, S.L. Molodtsov, D.V. Vyalykh, D.A. Vinokurov, V.P. Ulin, S.G. Konnikov, M.V. Shishkov, I.N. Arsentyev, I.S. Tarasov, Zh.I. Alferov, Concurrent investigations of electronic energy spectrum in A^3B^5-type nanostructures. // *Fiz. Tekhn. Poluprov*. **37**(8), p. 1017-1022 (2003) (in Russian).
16. M.G. Milvidsky, V.B. Osvensky, *Structural defects in epitaxial layers of semiconductors*. Metallurgiya, Moscow (1985) (in Russian).
17. I.N. Arsentyev, A.V. Bobyl, N.S. Boltovets, V.N. Ivanov, R.V. Konakova, Ya.Ya. Kudryk, O.S. Lytvyn, V.V. Milenin, I.S. Tarasov, A.E. Belyaev, E.V. Rusu, New manufacturing technology for InP epitaxial layers and properties of Schottky diodes made on their basis // In: *Proc. 14th intern. Crimean conference "Microwave & Telecommunication Technology" (CriMiCo'2004).* 13−17 Sept. 2004. Veber, Sevastopol (2004) p. 528-529.
18. E.H. Roderick, *Metal–semiconductor contacts*. Clarendon Press, Oxford (1978).

© 2005, V. Lashkaryov Institute of Semiconductor Physics, National Academy of Sciences of Ukraine